Journal of Hydrology 566 (2018) 846–859

Contents lists available at ScienceDirect

Journal of Hydrology

journal homepage: www.elsevier.com/locate/jhydrol

Research papers

Spatial-temporal changes in the longitudinal functional connectivity of river systems in the Taihu Plain, China

Xiaojun Deng[a,*], Youpeng Xu[b], Longfei Han[c], Song Song[d], Guanglai Xu[e], Jie Xiang[b]

[a] School of Economics, Zhejiang University of Finance & Economics, Hangzhou 310018, China
[b] School of Geographic and Oceanographic Science, Nanjing University, Nanjing 210023, China
[c] College of Resources and Environmental Sciences, Hunan Normal University, Changsha 410081, China
[d] School of Geographical Sciences, Guangzhou University, Guangzhou 510006, China
[e] School of Geography and Tourism, Anhui Normal University, Wuhu 241000, China

ARTICLE INFO

Keywords:
Longitudinal functional connectivity
Spatial-temporal changes
River systems
Water level
Taihu Plain

ABSTRACT

The longitudinal functional connectivity of river systems refers to the process-based connections between upstream and downstream areas and is fundamental to understanding the dynamic and nonlinear hydrological behaviour of river basins. However, the quantification of such connectivity remains a challenge due to the absence of a consensus on the appropriate data and methods, especially in delta plains. In this study, based on the difference between water level fluctuations at adjacent stations, a new and quantitative longitudinal functional connectivity index (LFCI) was developed for delta plains. Focusing on the Taihu Plain, we then analysed the spatial-temporal changes in the LFCI during 1960–2012 and investigated the correlations between the LFCI and climate change and human activities. We found that the decadal, annual and seasonal changes in the average LFCI all presented slightly increasing trends in the recent 50 period, but the annual average LFCI increased significantly after 1978; the average LFCIs in June, July, and August of the flood season were less than those in other months in the Taihu Plain. We also found that the spatial-temporal changes in the average LFCI exhibited larger differences at the subregional and station scales; those in the Wu-Cheng-Xi-Yu subregion were least, and the average LFCIs at stations near the borders of adjacent subregions were less than those at other stations. Moreover, we found that the average LFCI had significant correlations with precipitation, river density and water surface ratio. Our results were consistent with common sense facts, which demonstrated that the indicator developed in this study can quite effectively quantify the longitudinal functional connectivity of river systems in delta plains.

1. Introduction

Connectivity as a key term in hydrology, geomorphology and ecology, generally refers to the connections between different parts of a catchment, and their influences on water and sediment transfers and biological processes (Michaelides and Chappell, 2009). Although connectivity is regarded as an essential factor for ensuring species persistence, ecosystem integrity, and human well-being (Jaeger et al., 2014), it had not been introduced and studied as a broad and specific scientific question until the late 20th century (Bracken et al., 2013; Good et al., 2015).

Connectivity has also been broadly classified as hydrological connectivity, ecological connectivity, and geomorphological connectivity (Okin et al., 2015; Wohl et al., 2017; Lu et al., 2018). Of these types, hydrological connectivity is closely related to the transfer of matter, energy and organisms and to the physical, chemical and biological processes of river systems; the anthropogenic reduction in this property may result in major negative environmental effects (Pringle, 2003). Therefore, hydrological connectivity transcending different disciplines has received increasing interest, and how to quantify hydrological connectivity has become a research focus in the past decades (Michaelides and Chappell, 2009; Rinderer et al., 2018).

Hydrological connectivity is commonly grouped into two categories: (1) structural (or static) connectivity, which refers to spatial patterns of river systems and the extent of physical connections between rivers and lakes (Smith et al., 2010); and (2) functional (dynamic) connectivity, which refers to the interconnection of different areas in the same catchment by a process (Turnbull et al., 2008). The interaction of structural and functional connectivity is conducive to determining the dynamic and nonlinear hydrological behaviour (Michaelides and

* Corresponding author.
E-mail address: mijun45@163.com (X. Deng).

https://doi.org/10.1016/j.jhydrol.2018.09.060

Available online 29 September 2018
0022-1694/ © 2018 Published by Elsevier B.V.

Chappell, 2009). Although there are successful measures to quantify structural connectivity (e.g., topographic indices), standardized quantitative methods for functional connectivity are more rare due to the absence of a consensus on the appropriate data and methods (Bracken et al., 2013; Okin et al., 2015; Rinderer et al., 2018).

Meanwhile, hydrological connectivity can also be developed along the longitudinal dimension (e.g., from upstream to downstream areas), lateral dimension (e.g., from riparian/flood zones to river channel), and vertical dimension (e.g., from surface to subsurface) in addition to the temporal dimension (Amoros and Bornette, 2010; Covino, 2017). Among these dimensions, the longitudinal connectivity of river systems is extensively altered by anthropogenic impoundments and diversions throughout the world (Nilsson et al., 2005). However, the natural transfers of water and sediments and the regular migration of organisms are prevented by these transverse obstacles, resulting in important ecological consequences due to variations in the hydromorphological and biological conditions of the ecosystem (Solà et al., 2011). For the aforementioned reasons, longitudinal functional connectivity is more difficult to quantify than longitudinal structural connectivity (Chi et al., 2018; Ramulifho et al., 2018).

Unlike mountainous areas in sparsely populated upper basins (Caruso, 2015), delta plains are generally located in populous downstream zones. River systems in these regions are more vulnerable to interference by various human activities, and longitudinal functional connectivity is also easily altered by urbanization (Wohl et al., 2017). Even so, simulating longitudinal functional connectivity in these regions is still difficult because of the absence of sufficient data. Furthermore, research concerning a quantitative indicator of longitudinal functional connectivity in these regions is extremely rare. Therefore, developing a new indicator with currently available data is imperative to quantify longitudinal functional connectivity in delta plains.

The Taihu Plain is one of the most famous and rapidly urbanizing delta plain in China. However, a multitude of tributaries have been buried or diverted through pipes to increase the amount of land available for urbanization (Deng et al., 2015b). Meanwhile, innumerable floodgates have been constructed to protect against flooding, and the longitudinal functional connectivity of river systems has thus been partly weakened and even cut off by these human activities (Deng et al., 2018). The decrease in longitudinal functional connectivity of river systems along with the increase of extreme rainfall (Han et al., 2015) and pollutant discharge (Stone, 2011) complicates the hydrological cycle and nutrient exchange processes, finally resulting in more frequent flood disasters and serious water environmental pollution in the Taihu Plain (Duan et al., 2009; Wang et al., 2011). In recent years, these issues have gained increasing attention from the central and local governments. A growing number of water conservancy projects, including river channel dredging and returning farmland to lakes, have been executed to ease these crises. These protective projects not only partly restored the original connections between rivers and lakes but also established new links between originally unconnected rivers and lakes, eventually improving longitudinal functional connectivity. Therefore, investigating the spatial-temporal changes in longitudinal functional connectivity will assist in developing a further understanding of the correlations between hydrological connectivity and flood disasters and water pollution. Such investigations will provide support for making policies regarding flood disaster mitigation and water environmental protection in the Taihu Plain.

The goal of this study is to develop a new and quantitative indicator of longitudinal functional connectivity in delta plains and to analyse its spatial-temporal changes in the Taihu Plain. We first developed a longitudinal functional connectivity index (LFCI) based on major hydromorphological characteristics of delta plains and then employed several time series analysis methods including the moving average, linear trend, Mann-Kendall test (M-K), moving t-test (MTT), and Yamamoto method to analyse the spatial-temporal changes in the LFCI. Finally, we also investigated the correlations between the LFCI, climate change and human activities. The conclusions can improve the understanding of longitudinal functional connectivity in delta plains.

Fig. 1. Sketch map of the Taihu Plain.

2. Data and methods

2.1. Study area

The Taihu Plain is located in the centre of the Yangtze River delta in eastern China, covers an area of 15,757 km^2 and is 2–4 m above sea level. This region is known as Jiangnan Water Country due to the crisscrossing rivers and numerous lakes. The water surface area of 1590 km^2 occupies 9.72% of the total area, the total river length is 50,245 km, and the river density is 3.07 km/km^2 (Deng et al., 2015b). According to the landform conditions and river system distribution, this region can be divided into three subregions (Fig. 1): Wu-Cheng-Xi-Yu (WCXY), Yang-Cheng-Dian-Mao (YCDM), and Hang-Jia-Hu (HJH). Meanwhile, the Taihu Plain has always been a region with one of the most advanced economies and densest populations in China. Currently, the urbanization rate (the urban population as a percentage of the total population) has exceeded 50%, and the percentage of non-agricultural GDP is close to 100% in this region. However, rapid urbanization has given rise to serious pollution and flood disasters, and flood disaster mitigation tracking and water environmental protection have then become the key challenges for the future of the Taihu Plain (Liu et al., 2013).

2.2. Data sources

To analyse the changes in longitudinal functional connectivity through space and time, we collected the daily mean water level data at

Table 1
List of hydrological stations in the Taihu Plain.

Station name	Longitude (N)	Latitude (E)	Time series
Baishaoshan	120°07′	31°31′	1967–2012
Changzhou	119°59′	31°46′	1960–2012
Chenshu	120°32′	31°44′	1960–2012
Ganlu	120°35′	31°33′	1967–2012
Qingyang	120°15′	31°45′	1960–2012
Wuxi	120°13′	31°32′	1960–2012
Changshu	120°45′	31°38′	1960–2012
Chenmu	120°53′	31°11′	1962–2012
Guajingkou	120°39′	31°12′	1960–2012
Kunshan	120°58′	31°23′	1971–2012
Pingwang	120°38′	31°00′	1967–2012
Suzhou	120°39′	31°17′	1961–2012
Xiangcheng	120°44′	31°29′	1960–2012
Zhitang	120°01′	31°33′	1977–2012
Gongchenqiao	120°08′	30°20′	1960–2012
Tangxi	120°11′	30°29′	1960–2012
Wangjiangjing	120°43′	30°53′	1960–2012
Linghu	120°11′	30°43′	1960–2012
Xiashi	120°41′	30°31′	1960–2012
Wuzhen	120°30′	30°45′	1960–2012
Yuhang	119°56′	30°17′	1960–2012
Jiaxing	120°42′	30°45′	1960–2012
Sanliqiao	120°07′	30°51′	1971–2012
Xincheng	120°37′	30°48′	1967–2012
Tongxiang	120°32′	30°38′	1971–2012
Yucheng	120°51′	30°32′	1965–2012
Shuanglin	120°21′	30°47′	1968–2012
Nianyukouzha	120°04′	30°40′	1965–2012
Jingshanzha	120°04′	30°43′	1964–2012
Huanlouzha	120°15′	30°56′	1964–2012

30 hydrological stations in the Taihu Plain from 1960 to 2012. All hydrological stations are located on the main nodes of river systems and have long-term continuous data. Meanwhile, the observations at these stations can characterize the changes in water levels of main rivers or lakes, which are closely related to the water levels at the surrounding stations. The spatial distribution and time series lengths of the stations are displayed in Fig. 1 and Table 1. To analyse the natural and human factors related to longitudinal functional connectivity changes, we also collected the daily precipitation at the aforementioned 30 hydrological stations in the Taihu Plain from 1960 to 2012. In addition, we extracted river system data for the study area from 1:50,000 topographic maps published in the 1960s, 1980s, and 2010s and obtained floodgate data for the Taihu Plain from the First National Water Resources Census in China in 2012.

2.3. Longitudinal functional connectivity index (LFCI)

As mentioned previously, the longitudinal functional connectivity of river systems refers to the process-based connection between upstream and downstream areas in river basins and includes the water-mediated linkages between different rivers (or lakes), different parts of the same river (or lake), and rivers and lakes. In other words, the longitudinal functional connectivity of river systems can be regarded as the capability for internal and external water exchange between rivers and lakes. However, the water level is more suitable than the stream flow as a hydrological parameter to measure the capability for water exchange in delta plains, because the latter in these regions are slower and more variable than those in other catchments. Meanwhile, the distinctive hydromorphological characteristics of these regions (e.g., flat terrain and crisscrossing rivers) are also conducive to establishing a response relationship between adjacent stations by water level. The response relationship of water levels between adjacent stations (Bracken and Croke, 2007; Cabezas et al., 2011) can characterize the longitudinal functional connectivity of river systems in delta plains.

In this study, we attempt to develop a longitudinal functional connectivity index (LFCI) according to the water level fluctuation differences between adjacent stations. The fundamental principle of this indicator is described as follows: a smaller difference between water level fluctuations at adjacent stations at the same time (daily scale) is indicative of a more positive longitudinal functional connectivity; otherwise, a smaller longitudinal functional connectivity is indicated. These relations can be expressed as follows:

$$LFCI = \frac{1}{\Delta L_{ab}} = \frac{1}{[(L_{ai}-L_{aj})-(L_{bi}-L_{bj})]} \quad (1)$$

where ΔL_{ab} is the difference between water level fluctuations at adjacent stations a and b; and L_{ai}, L_{aj}, L_{bi}, and L_{bj} are the water levels of adjacent stations a and b at times i and j, respectively. However, the formula has no mathematical meaning when $\Delta Lab = 0$, and the water level fluctuations at most stations are in the second decimal place or smaller. Therefore, in this paper, the aforementioned formula is improved as follows:

$$LFCI = \frac{0.1}{\Delta L_{ab} + 0.1} = \frac{0.1}{[(L_{ai}-L_{aj})-(L_{bi}-L_{bj})] + 0.1} \quad (2)$$

It is clear that LFCI is negative when $\Delta Lab < -0.1$. To achieve horizontal and vertical comparisons in space and time and to constrain LFCI within [0, 1], the formula is rewritten as shown below:

$$LFCI = \frac{1}{10 \times |\Delta L_{ab}| + 1} = \frac{1}{10 \times |(L_{ai}-L_{aj})-(L_{bi}-L_{bj})| + 1} \quad (3)$$

where $0 < LFCI \leq 1$; the longitudinal functional connectivity is the strongest when $LFCI = 1$ and is more weaker when $LFCI$ is close to 0.

To analyse the temporal and spatial changes in longitudinal functional connectivity in the Taihu Plain, we first calculated all daily average LFCIs between any two adjacent stations and then calculated the regional, subregional and station LFCIs at monthly, seasonal, annual and decadal scales. Specifically, a regional LFCI is the average of LFCIs of any two adjacent stations in the Taihu Plain, a subregional LFCI is the average of LFCIs of any two adjacent stations in the subregion, and the LFCI at a single station is the average of LFCIs between this station and all of its adjacent stations. Moreover, monthly, seasonal, annual and decadal LFCIs at certain spatial scales are the averages of regional, subregional or station daily LFCIs at these temporal scales.

As mentioned, water levels are the only available hydrological data in delta plains, and their changes can reliably reflect the hydrological process. Hence, the developed functional connectivity indicator based on the response of water levels between adjacent stations has the advantages of available data, simple computation, favourable maneuverability and easy understanding and is particularly suitable for the hydrological characteristics of delta plains.

2.4. Time series analysis methods

As mentioned, the development of the LFCI is based on water levels at the hydrological stations. Consequently, the LFCI can be regarded as a random variable in time as with the water level of a river network. Similarly, the LFCI can be investigated by using general analysis methods for hydrological time series. Generally, hydrological time series are influenced by climate change and human activities. To distinguish and quantify the effect of human activities, trend test methods are frequently used to identify abrupt change points that cause inconsistent changes in hydrological time series (Ma et al., 2008; Xie et al., 2018). For this reason, we employed a moving average and a linear trend to analyse the variation trend of the LFCI and used the M-K test, MTT, and Yamamoto method to identify abrupt changes in the LFCI.

2.4.1. Moving average

A moving average is approximately equivalent to a low pass filter and can significantly weaken cycles shorter than the moving length in a time series (Wu et al., 2009). The moving average series of a time series

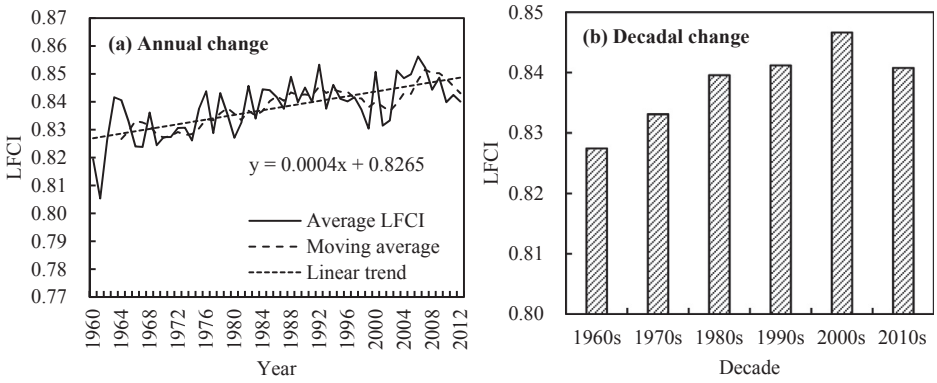

Fig. 2. Annual and decadal changes in the average LFCIs in the Taihu Plain.

$x_1, x_2, x_3, \ldots, x_n$ can be expressed as:

$$\hat{x}_j = \frac{1}{k}\sum_{i=1}^{k} x_{i-j-1}, \quad j = 1, 2, \cdots, n-k+1 \tag{4}$$

where k is the moving length, and k is generally an odd bumber. In this study, $k = 5$ was adopted.

2.4.2. Linear trend

Generally, the linear trend of a time series can be estimated by the least square method and expressed by a linear regression equation as (Tang et al., 2011):

$$x_i = a + bt_i, \quad i = 1, 2, \cdots, n \tag{5}$$

where x_i is the response variable; t is the time variable; a is a constant; b is the estimated coefficient, and the trend is negative when $b < 0$ but positive when $b > 0$.

2.4.3. Mann-Kendall test (M-K)

The M-K test is a non-parametric statistical test method widely used to identify variation trends in hydrologic and meteorological series (Yaghmaei et al., 2018). For time series $x_1, x_2, x_3, \ldots, x_n$, the M-K rank statistic S_k can be expressed as follows:

$$S_k = \sum_{i=1}^{k} r_i, \quad k = 1, 2, \cdots, n \tag{6}$$

where $r_i = 1$ when $x_i > x_j$ and $r_i = 0$ when $x_i \le x_j$.

Under the null hypothesis where no trend is assumed, the statistic UF_k is defined as follows:

$$UF_k = \frac{[S_k - \mathrm{E}(S_k)]}{\sqrt{\mathrm{var}(S_k)}}, \quad k = 1, 2, \cdots, n \tag{7}$$

where $UF_1 = 0$; and $\mathrm{E}(S_k)$ and $\mathrm{var}(S_k)$ are the expected value and variance, respectively, and are written as follows:

$$\begin{cases} E(S_k) = \frac{n(n+1)}{4} \\ var(S_k) = \frac{n(n-1)(2n-5)}{72} \end{cases} \tag{8}$$

Based on the inverse series $x_n, x_{n-1}, x_{n-2}, \ldots, x_1$, the aforementioned process can be repeated, and $UB_k = -UF_k$ ($k = n, n-1, n-2, \ldots, 1$) and $UB_1 = 0$ are also defined.

If the intersection point of the UB_k curve and the UF_k curve is located between the confidence lines (95% is widely accepted), this point can be regarded as a time point of abrupt change.

2.4.4. Moving t-test (MTT)

The MTT is widely used to detect the difference between the averages of two groups of samples (Liang et al., 2011). For a time series x with n samples, the statistic t can be expressed as follows:

$$t = \frac{\bar{x}_1 - \bar{x}_2}{\sqrt{\frac{n_1 s_1^2 + n_2 s_2^2}{n_1 + n_2 - 2}} \times \sqrt{\frac{1}{n_1} + \frac{1}{n_2}}} \tag{9}$$

where n_1 and n_2 are the sizes of x_1 and x_2 subsamples, respectively, and $n_1 = n_2$ is widely accepted; $\bar{x}_1$, $\bar{x}_2$ and S_1^2, S_2^2 are the averages and variances of the subsamples.

If the absolute value of t is less than the critical value for the confidence level a (t_a), there is no significant difference between the averages of the two subsamples. In contrast, an abrupt change is believed to exist in the total sample when $t \ge t_a$.

2.4.5. Yamamoto method

Similar to the goal of the MTT method, that of the Yamamoto method is also to identify an abrupt change based on the difference between the averages of two subsamples (Zhao et al., 2008). According to the averages ($\bar{x}_1$ and $\bar{x}_2$) and variances (S_1^2 and S_2^2) of two subsamples, the signal to noise ratio (SNR) can be defined as follows:

$$SNR = \frac{|\bar{x}_1 - \bar{x}_2|}{s_1 + s_2} \tag{10}$$

If $n_1 = n_2 = 10$, a $SNR = 1.0$ means that the absolute value of the statistic t is larger than the critical value for the confidence level $a = 0.05$; i.e., there is significant abrupt change in the sample.

3. Results

3.1. Regional change in longitudinal functional connectivity

As shown in Fig. 2, the average LFCI is 0.84 in the Taihu Plain in the recent 50 period, and the annual and decadal changes in LFCI are insignificant. In spite of this result, the ideal value of the LFCI should be 1 because a flat topography and crisscrossing rivers provide favourable conditions for better connectivity in this region. The annual average LFCI has a slightly increasing trend (0.0004/a) but shows a more significant decreasing tendency since 2006 (0.0033/a). Similarly, the difference between decadal LFCIs is small, and these values also show a trend of first increasing and then decreasing. Therefore, longitudinal functional connectivity must be improved because its status is not the best in the Taihu Plain, especially given its degradation trend in recent years.

According to the hydrological regime in the Taihu Plain, the five months from May to September in each year are regarded as the flood season, and the other months are regarded as the non-flood season. On this basis, the average LFCIs in the flood and non-flood seasons can be obtained. As shown in Fig. 3, the average LFCIs in the flood and non-flood seasons all present slightly increasing trends in the recent 50 period, and the increment rate in the flood season (0.0006/a) is twice that in the non-flood season (0.0003/a). Meanwhile, the average LFCI is 0.82 in the flood season, but it is 0.86 in the non-flood season. In other

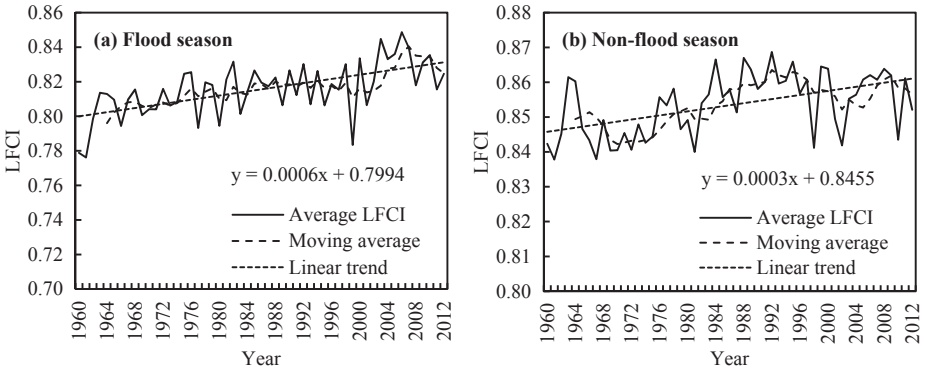

Fig. 3. Seasonal changes in the average LFCI in the Taihu Plain.

words, the longitudinal functional connectivity in the non-flood season is better than that in the flood season, although the improvement in the latter is greater than that in the former. Hence, longitudinal functional connectivity must be further improved in the flood season.

By comparison, the average LFCIs in the first two months and last three months of the year are all greater than 0.85, but those in June, July and August are less than 0.81 (Fig. 4). Meanwhile, there are also increasing trends in the average LFCIs in each month, but their increment rates present larger differences. The largest increment rate is 0.001/a in September, but the lowest increment rate is only 0.00002/a in January. Meanwhile, the increment rates are less than 0.0004/a in June, July and August. In summary, the average values and increment rates of LFCIs in June, July and August are all smaller than those in other months, and so longitudinal functional connectivity must be improved preferentially in June, July and August.

3.2. Subregional changes in longitudinal functional connectivity

To analyse the spatial-temporal changes in longitudinal functional connectivity in the Taihu Plain, the average LFCI during 1960–2012 in each subregion is calculated. The results indicate that the average LFCI in WCXY is 0.80 and those in YCDM and HJH are 0.87 and 0.84, respectively. Therefore, the longitudinal functional connectivity in YCDM is the most positive, but that in WCXY is the least in the Taihu Plain. This result implies that WCXY is the key subregion for improving longitudinal functional connectivity in the Taihu Plain.

Similarly, the annual average LFCIs in each subregion presents slightly increasing trends, but the increment rates present larger differences (Fig. 5). Specifically, the increment rate of the annual average LFCI in YCDM is 0.0001/a, which is only one-third that of HJH (0.0003/a), and one-ninth that of WCXY (0.0009/a). Meanwhile, the five-year moving average curve for the annual average LFCI indicates that longitudinal functional connectivity decreases first and then increases in WCXY, but the changes are alternate increases and decreases in YCDM and HJH. In addition, the decadal average LFCI in WCXY decreases first and then increases, but those in YCDM and HJH manifest inverse change trends. These results indicate that longitudinal functional connectivity in YCDM and HJH presents decreasing trends in recent decades, emphasizing that longitudinal functional connectivity must also be improved in these subregions.

There are also large differences in the changes in LFCIs between the flood season and non-flood season in each subregion (Fig. 6). The average LFCIs in both the flood season and non-flood season present a slightly increasing trend in WCXY, and the increment rate is 0.001/a. Meanwhile, the five-year moving average curves in these two periods also present first a decreasing and then an increasing trend, but the fluctuation range in the flood season is less than that in the non-flood season. In contrast, the average LFCI in the flood season presents a slightly decreasing trend in YCDM, but that in the non-flood season presents a slightly increasing trend, and the increment rate in the non-flood season is twice the decrement rate in the flood season. Moreover, the average LFCI in HJH in the flood season presents a slightly increasing trend, but that in the non-flood season exhibits a slightly decreasing trend, and the decrease rate in the non-flood season is extremely small. Thus, longitudinal functional connectivity improvement is recommended in the flood season in YCDM, but in the non-flood season in HJH.

As shown in Fig. 7, the three subregions have a common characteristic; i.e., the monthly average LFCI in each subregion presents first a decreasing and then an increasing trend. The result indicates that the longitudinal functional connectivity in June, July and August is worse than that in other months in the three subregions. Meanwhile, the monthly average LFCI in YCDM is the largest, but that in WCXY is the smallest. In addition, the changes in the monthly average LFCIs in the three subregions show larger differences. The average LFCI in each month all present different increasing rates in WCXY, but those in

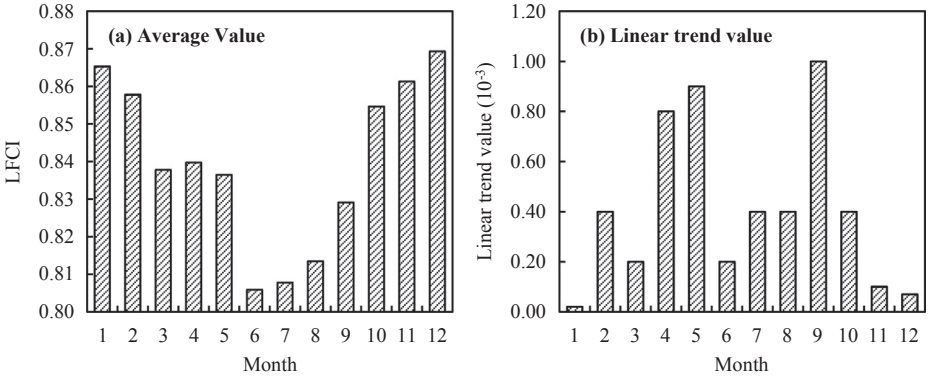

Fig. 4. Monthly changes in the average LFCI in the Taihu Plain.

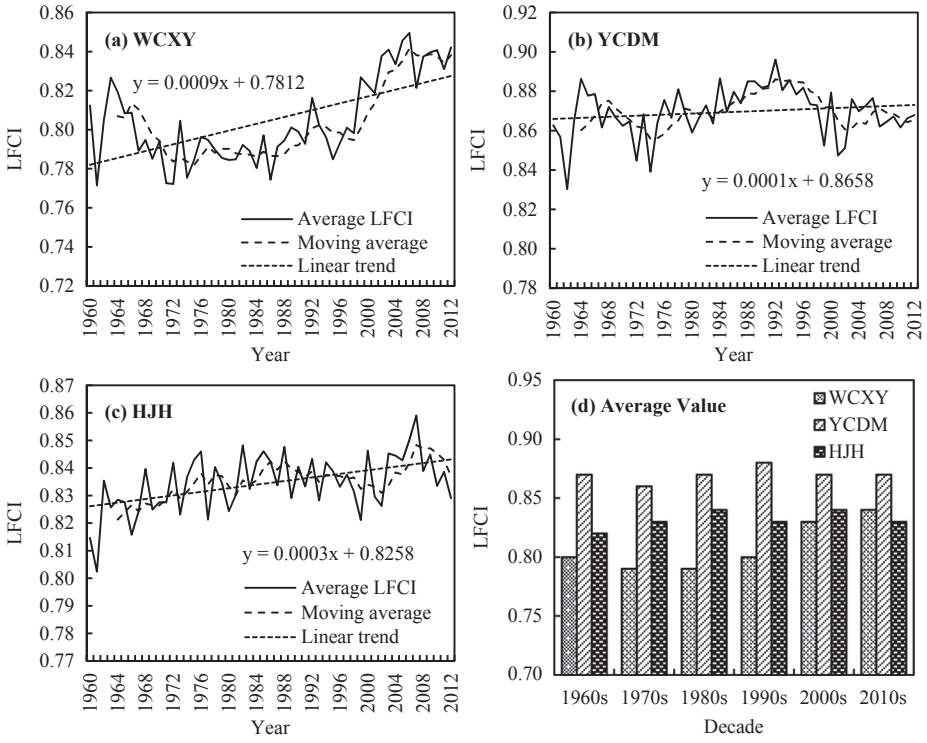

Fig. 5. Annual and decadal changes in the average LFCI in each subregion.

YCDM and HJH also exhibit various decreasing magnitudes. Specifically, a decreasing trend is observed in June, July and August in YCDM but is seen in the first three months and the last two months in HJH. In summary, longitudinal functional connectivity improvement is strongly needed in June, July and August in YCDM and in the first three months and last two months in HJH.

3.3. Station changes in longitudinal functional connectivity

As shown in Fig. 8, the LFCIs of 83.33% of the stations exceed 0.81, and the LFCIs of 13.33% of the stations are between 0.71 and 0.80, but LFCIs of 3.33% of the stations are less than 0.60. Meanwhile, the smaller annual average LFCIs are mainly present at those stations near the border between the Taihu Plain and the western mountain subregion or the Taihu Lake subregion, implying that longitudinal functional connectivity of those stations near the border between adjacent subregions must be improved preferentially.

Similarly, there are insignificant differences between the linear trend values of the annual average LFCI at each station (Fig. 8, Table 2). The linear trend value is less than 0.001 at 86.67% of the stations, and the maximum is only 0.0032/a, while the minimum is less than 0.00001/a. Meanwhile, the annual changes in the average LFCI present a slightly increasing trend at 76.67% of the stations; only 7 stations have slightly decreasing trends, and they are mainly located near the border between the Taihu Plain and the western mountain subregion. Moreover, stations with slightly decreasing trends are also distributed near the border between YCDM and WCXY (or HJH). These results indicate that longitudinal functional connectivity of the critical stations near the borders between adjacent subregions should be given more attention and improved.

As shown in Fig. 9, most of the decadal average LFCIs are between 0.81 and 0.90. Meanwhile, the LFCI at Jingshanzha is greater than 0.90 in the 1960s; at Wangjiangjing, in the 1970s and 2000s; and at Yucheng, in the 2000s, but the LFCI is less than 0.60 at Yuhang. In addition, the decadal average LFCIs in those stations near the border between YCDM and WCXY (or HJH) also indicate a decreasing trend. As an example, the decadal average LFCI at Nianyukouzha decreases from 0.82 in the 1960s to 0.78 in the 2010s. Therefore, longitudinal functional connectivity at those stations near the border between adjacent subregions must be improved.

However, there are certain spatial differences in the average LFCIs in the flood and non-flood seasons (Fig. 10). The average LFCIs in the flood season are between 0.71 and 0.80 in WCXY but between 0.81 and 0.90 in YCDM. Meanwhile, the average LFCIs at 68.75% of the stations in HJH are between 0.81 and 0.90 and at the rest of the stations are between 0.71 and 0.80. These results indicate that the average LFCI in the flood season is the least in WCXY, but it is the most positive in YCDM. Although the average LFCI in the non-flood season is still between 0.81 and 0.90 at each station in YCDM, it is also greater than 0.80 at each station in WCXY except Baishaoshan. Compared with values in the flood season, the average LFCI in the non-flood season also exceeds 0.80 at Nianyukouzha and Tangxi in HJH and is even greater than 0.90 at Wangjiangjing. Overall, the average LFCI during the non-flood season is more positive than that during the flood season. Thus, the longitudinal functional connectivity at the stations in the flood season in WCXY must be improved first.

3.4. Abrupt changes in longitudinal functional connectivity

According to the basic step of the M-K test, we can draw the curves of UF and UB for the annual average LFCI in the Taihu Plain and two straight dashed lines representing the 95% confidence interval (Fig. 11). The curves of UF and UB intersect in 1978, which indicates that there is a significant increasing trend in the annual average LFCI in the Taihu Plain after 1978. Meanwhile, the UF curve continues the increasing trend and substantially exceeds the critical line of the 95% confidence interval after 1982, which indicates that the increasing trend of the annual average LFCI in the Taihu Plain is extremely significant after 1982. Moreover, the abrupt change type of the annual average LFCI observed in the Taihu Plain is a mean value abrupt change; i.e., the annual average LFCI increases to 0.84 during 1978–2012 from 0.83 during 1960–1977. This abrupt change point in

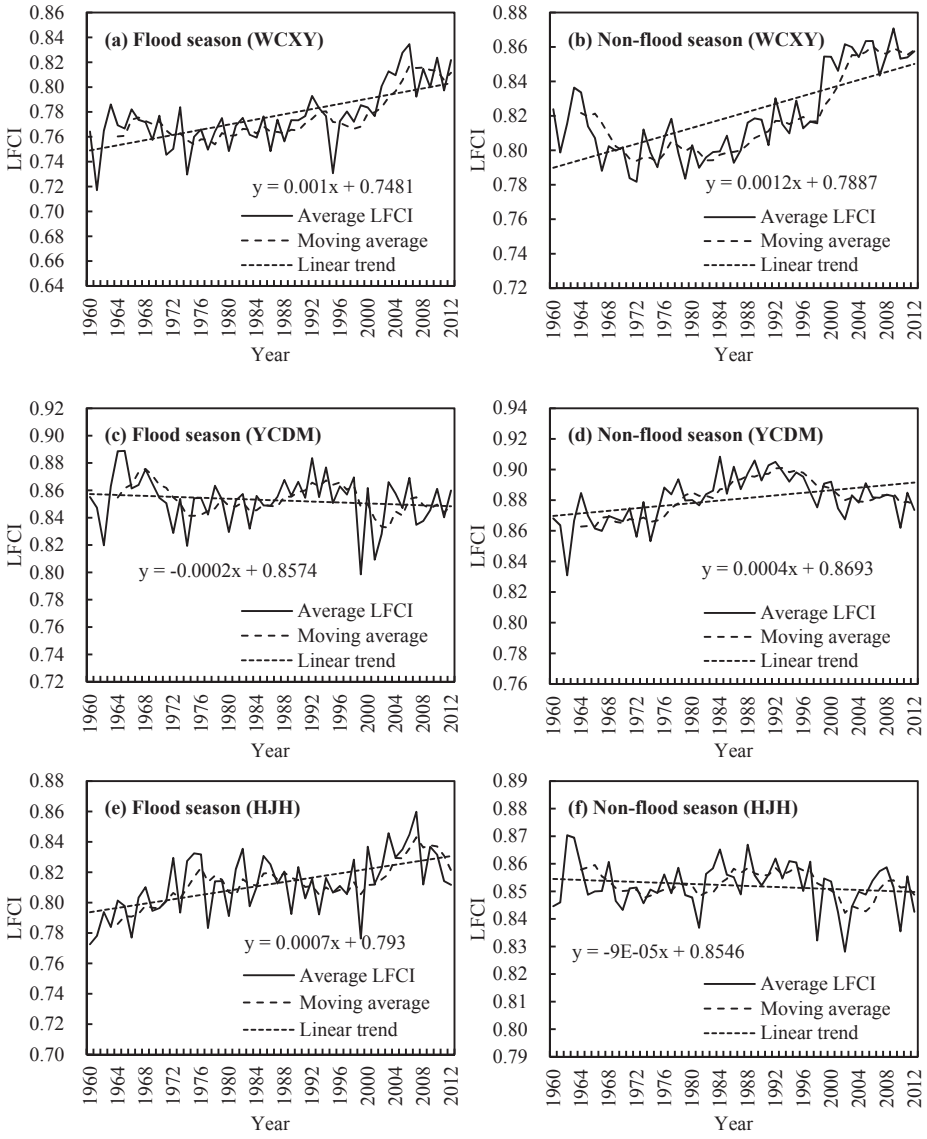

Fig. 6. Seasonal changes in the average LFCI in each subregion.

longitudinal functional connectivity is consistent with the beginning of the rapid urbanization in the Taihu Plain, which indicates that longitudinal functional connectivity is more sensitive to human activities than to climate change and other factors in this region.

Similarly, the abrupt change times for the annual average LFCI in WCXY and HJH can be confirmed as 2001 and 1971, respectively (Fig. 12). However, there are four intersection points (1963, 1971, 2010 and 2011) between the 95% confidence level lines in YCDM. Confirming these four intersection points as abrupt change points is difficult. Therefore, the MTT and Yamamoto method are employed to analyse the true abrupt point, and a decade is confirmed as the length of each subsample. As shown in Fig. 12(d)–(f), 1984 and 1998 are both abrupt change points in YCDM; the former is the abrupt change point from decreasing to increasing, but the latter is the opposite. These results indicate that the time points of connectivity improvement in the three subregions are inconsistent. In fact, the rehabilitation and reconstruction of river systems were generally carried out step by step and according to plan. To discharge floods in the Taihu Plain and prevent water from entering Shanghai, these positive projects were widely constructed in HJH before the 1980s. With the rapid development of the social economy in Suzhou, Wuxi and Changzhou, the focus of these constructions migrated gradually to YCDM in the 1980s and to WCXY in the 2000s (Deng et al., 2015b). In addition, the annual average LFCI in YCDM presents significant degradation since 1998. A probable cause is that there were more disruptive human activities than the aforementioned protective human activities during the rapid urbanization, such as the burying of tributaries and the embezzlement of lakes.

According to the three aforementioned methods, the abrupt change time points for the annual average LFCI in each station can be confirmed as shown in Table 3. The abrupt change time points for the annual average LFCI at each station are obviously different. Specially, the times and trends of abrupt change at 80% of the stations are almost consistent with those in their subregion, and 20% of the stations show earlier change times and opposite change trends in WCXY. Meanwhile, in YCDM, only 37.5% of the stations exhibit times and trends of abrupt change that are nearly identical to those of their subregion; 50% of the stations show only one change point at different change times, but 12.5% of the stations display extremely inconsistent change times and completely opposite change trends. In addition, in HJH, only 18.75% of the stations exhibit times and trends of abrupt change similar to those of their subregion; 31.25% of the stations show similar change trends but different change times, and 6.25% of the stations display similar change times but opposite change trends; 18.75% of the stations

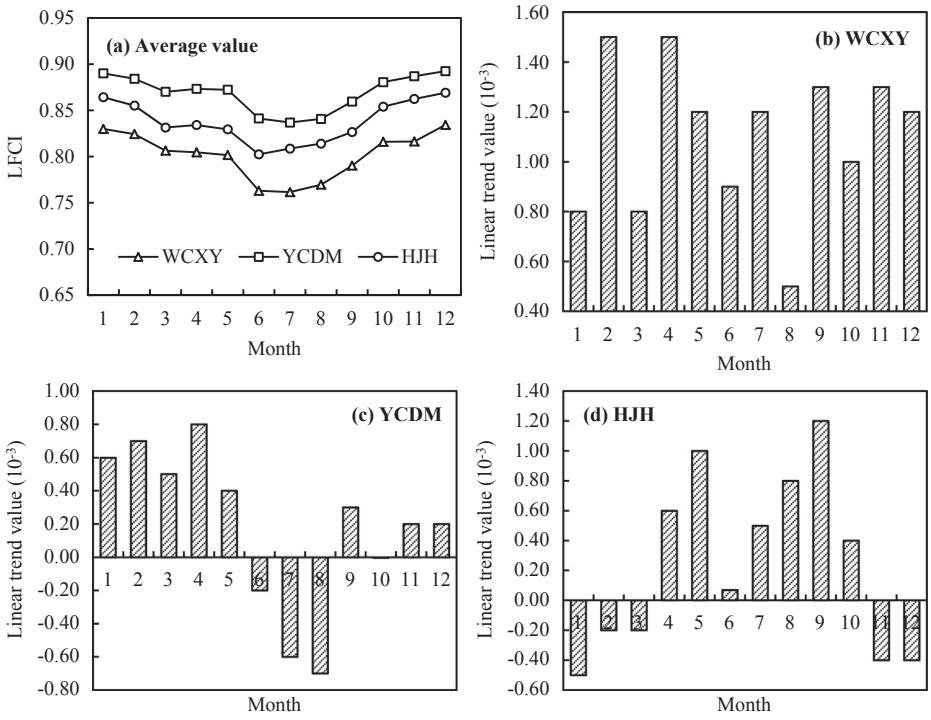

Fig. 7. Monthly changes in the average LFCI in each subregion.

manifest different change times and opposite change trends, but 25% of the stations present two change points and different change trends.

In general, the abrupt change times and trends of the annual average LFCIs at each station in WCXY are nearly consistent with those within the subregion, but the times and trends exhibit significant differences in YCDM, and the internal differences in HJH are more significant. One reason for this pattern might be that the beginnings of extensive positive or negative human activities at each station were

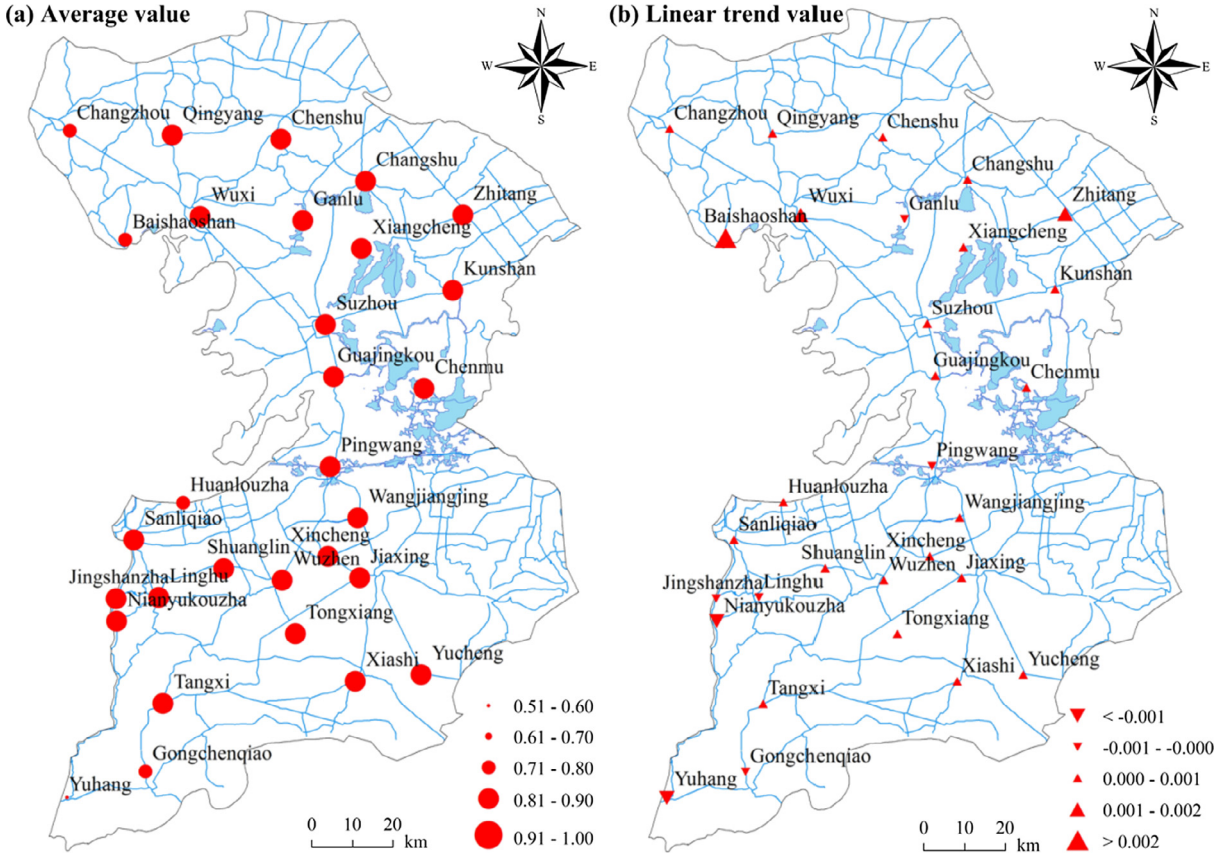

Fig. 8. Annual average and linear trend values of the average LFCI at each station.

Table 2
Linear trend values of the annual average LFCIs at each station.

Station	Linear trend value	Station	Linear trend value	Station	Linear trend value
Baishaoshan	0.0032	Kunshan	0.0008	Xiashi	0.0006
Changzhou	0.0005	Guajingkou	0.0005	Shuanglin	0.0005
Qingyang	0.0008	Chenmu	0.0003	Linghu	−0.0004
Wuxi	0.0011	Pingwang	−0.0001	Huanlouzha	0.0010
Chenshu	0.00001	Wangjiangjing	0.0003	Sanliqiao	0.0005
Ganlu	−0.0007	Jiaxing	0.0004	Jingshanzha	−0.0009
Changshu	0.0002	Xincheng	0.0006	Nianyukouzha	−0.0010
Zhitang	0.0016	Wuzhen	0.0005	Tangxi	0.0002
Xiangcheng	0.0001	Tongxiang	0.0004	Gongchenqiao	−0.0003
Suzhou	0.0003	Yucheng	0.0002	Yuhang	−0.0012

asynchronous across the Taihu Plain, but these activities began at relatively consistent times in WCXY due to unified planning and management.

3.5. Correlations between longitudinal functional connectivity and climate change and human activities

As a kind of hydrological connectivity, longitudinal functional connectivity is also affected by climate change and human activities (Pumo et al., 2017; Ala-aho et al., 2018). Among these changes, precipitation is one of the most important indicators used to detect climate change (Liang et al., 2011), and the modification of river systems and construction of dams and floodgates are two important human activities that impact hydrological connectivity (Deng et al., 2018; Karim et al., 2015). Thus, we employed the annual precipitation (AP) and average LFCI at each station from 1960 to 2012 to analyse the correlation between climate change and longitudinal functional connectivity. Limited by the available information, we collected only river system data from the 1960s, 1980s, and 2010s, and floodgate data in 2012. To achieve

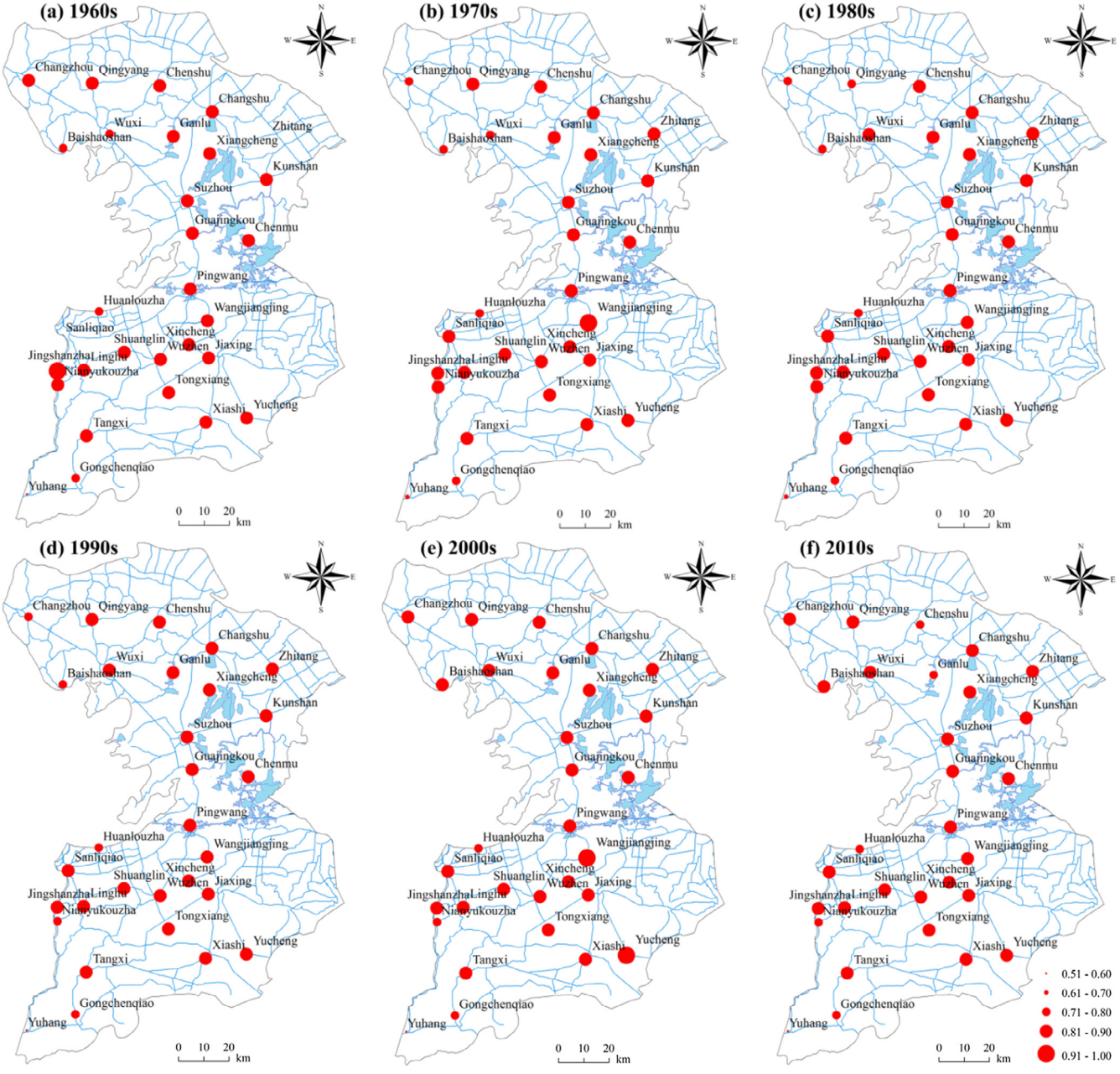

Fig. 9. Decadal changes in the average LFCI at each station.

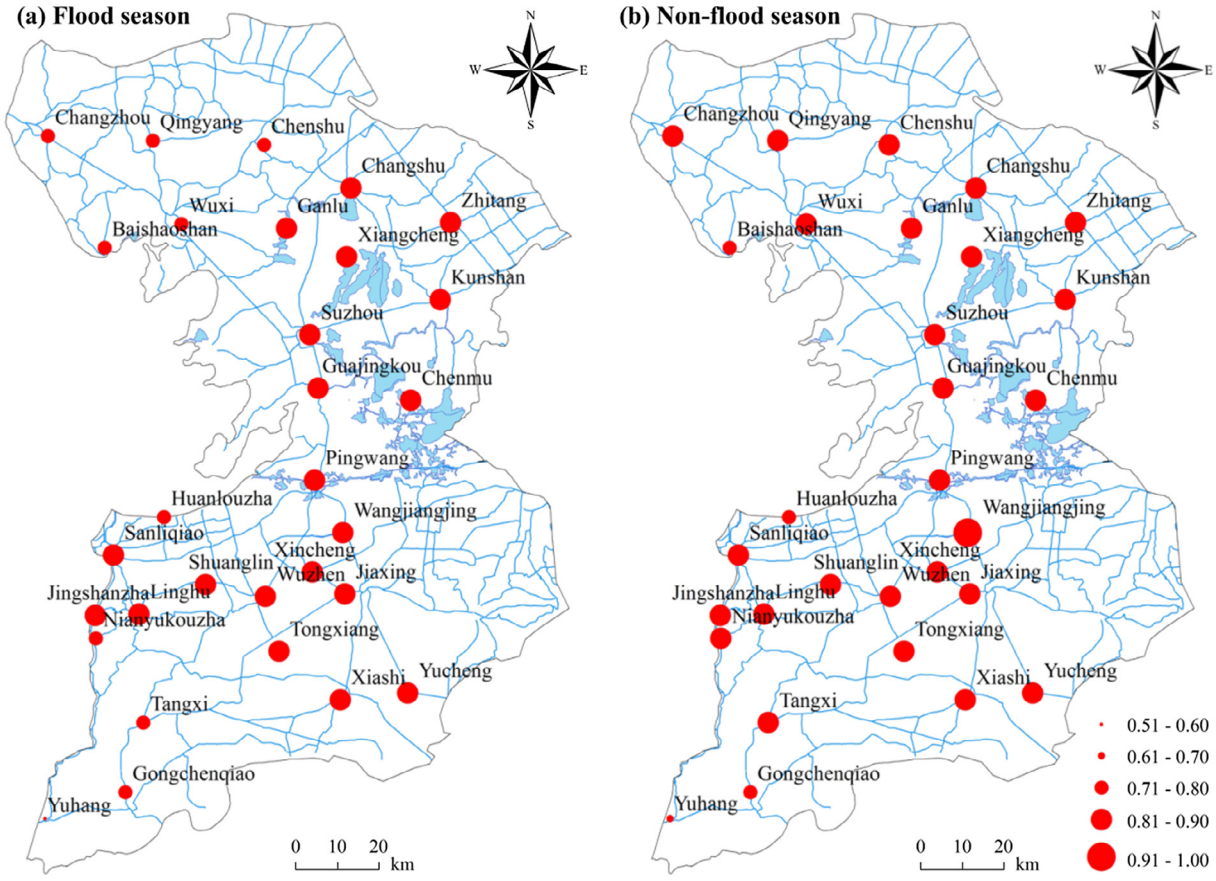

Fig. 10. Seasonal differences between the average LFCIs at each station.

consistency among hydrology, river system characteristics, and floodgate data, we generated a 20 km buffer around each station according the mean distance between every two adjacent stations. Then, we calculated the number of floodgates (N_f) and four common river system characteristic indicators in each buffer, including river density (D_r, the ratio of the total length of river to the buffer area), water surface ratio (W_p, the ratio of the total area of rivers and lakes at the mean water level to the buffer area), river development coefficient (K_ω, the ratio of the total length of tributaries to that of the main river in a buffer), and main river area length ratio (R_m, the ratio of area and length of the main river in a buffer). Finally, we employed the average LFCI at each station and the river system characteristic indicators for each station buffer in the 1960s, 1980s, and 2010s to detect the correlations between longitudinal functional connectivity and river system characteristics, and we used the average LFCI and N_f for each station buffer in 2012 to analyse the correlation between longitudinal functional connectivity and floodgates.

As presented in Table 4, the Pearson correlation coefficient between LFCI and AP is negative and significant at the 0.01 level. This result indicates that longitudinal functional connectivity significantly increases with decreasing precipitation. The correlation is also consistent with an aforementioned result; i.e., that longitudinal functional connectivity of the flood season is less than that of the non-flood season. Meanwhile, the Pearson correlation coefficients between the LFCI and the four river system characteristic indicators are all positive, and the correlations are significant at the 0.01 level for D_r and W_p. The results indicate that longitudinal functional connectivity increases with increases in these four indicators. This phenomenon is extremely significant for river density and water surface ratios. These results also demonstrate that there exists significant spatial heterogeneity in the

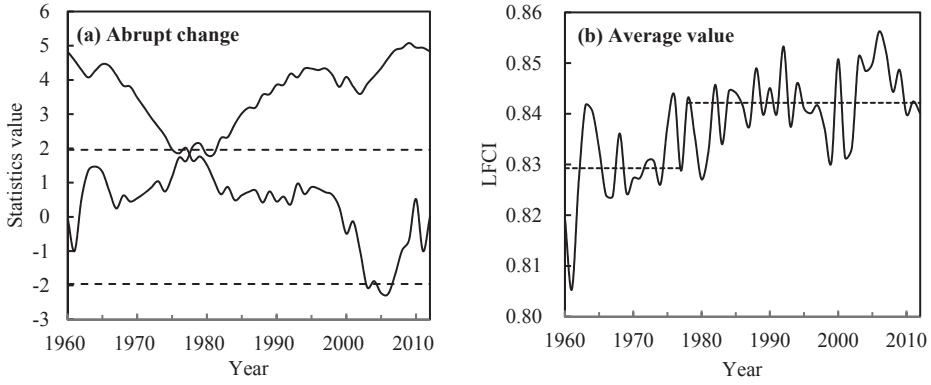

Fig. 11. Abrupt changes in the annual average LFCI in the Taihu Plain.

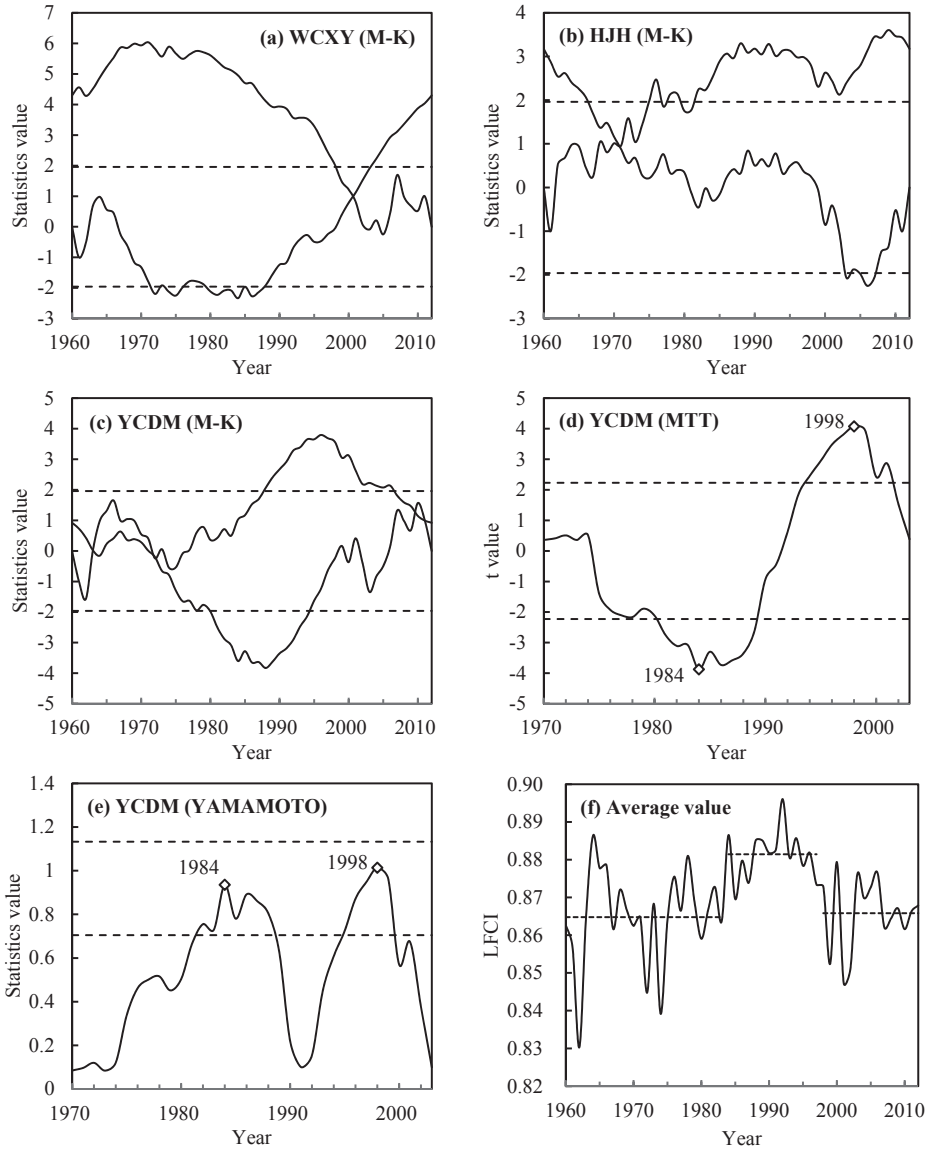

Fig. 12. Abrupt changes in the annual average LFCI in each subregion.

Table 3
Abrupt changes in the annual average LFCIs at each station.

Station	Time and trend	Station	Time and trend	Station	Time and trend
Baishaoshan	1998↑	Kunshan	1988↑	Xiashi	1990↑
Changzhou	2001↑	Guajingkou	1986↑, 1996↓	Shuanglin	1988↑
Qingyang	2001↑	Chenmu	1975↑	Linghu	1971↓
Wuxi	1998↑	Pingwang	1994↓, 2002↑	Huanlouzha	1973↑
Chenshu	1982↑	Wangjiangjing	1971↑	Sanliqiao	1992↓, 2002↑
Ganlu	1998↓	Jiaxing	1977↑	Jingshanzha	1977↓
Changshu	1984↑, 1999↓	Xincheng	1983↓, 2002↑	Nianyukouzha	1989↓
Zhitang	1989↑	Wuzhen	2002↑	Tangxi	1972↓, 1983↑
Xiangcheng	1984↑, 2001↓	Tongxiang	2000↑	Gongchenqiao	1981↑, 1991↓
Suzhou	1977↑	Yucheng	2000↑	Yuhang	1989↓

Table 4
Pearson correlations between LFCI and precipitation, river system characteristics, and floodgates.

	Precipitation	River system characteristics				Floodgates
	AP	D_r	W_p	K_ω	R_m	N_f
LFCI	−0.1769***	0.5041***	0.4373***	0.0183	0.2136	0.4110

*** Note: Correlation is significant at the 0.01 level.

changes in longitudinal functional connectivity, similar to that for the non-synchronous changes in river systems in time. Moreover, the Pearson correlation coefficient between the LFCI and N_f is positive but not significant at the 0.01 level, which indicates that longitudinal functional connectivity increases with an increasing number of floodgates. The insignificant correlation is possibly caused by neglecting the controlling rule of these floodgates due to the limitations of the data used in this study. To discharge floods during the flood season or improve the water quality in the non-flood season, anthropogenic water exchange by water pumps significantly increases the longitudinal functional connectivity between areas inside and outside of floodgates.

4. Discussions

4.1. Indicators of longitudinal functional connectivity

The term "longitudinal functional connectivity" is widely seen as a process-based hydrological connectivity from upstream to downstream areas, but its applicability is always disputed. The main contention is whether longitudinal functional connectivity can be quantitatively described by many indicators (Antoine et al., 2009; Troch et al., 2009). Currently, although the concept of longitudinal functional connectivity is resonated with the wider public, selecting one or more representative indicators to describe longitudinal functional connectivity variations remains an essential problem (Bracken et al., 2013).

In recent decades, many indicators concerning catchment topography, soil moisture, and solute travel times have been developed and applied to longitudinal functional connectivity assessment (Bracken et al., 2013). However, some potential problems, such as topographic factors and data requirements make these indicators inapplicable in many regions. In addition, the change in water level is often regarded as a characteristic of the hydrological process in delta plains. Therefore, the response relations of water levels between adjacent stations (Bracken and Croke, 2007; Cabezas et al., 2011) can be employed to characterize longitudinal functional connectivity in delta plains.

In this study, a new and quantitative indicator (LFCI) was developed to describe longitudinal functional connectivity in delta plains. Based on the differences between water level fluctuations at adjacent stations, this indicator can dynamically reflect the hydrological processes between adjacent river channels or different parts of the same river channel. Another advantage of the developed indicator is its lower data requirement; i.e., only water level data are needed, and these data are easy to obtain because of the widespread use of hydrological stations. Moreover, this indicator relies on easily operated and convenient calculations, which are two other advantages.

However, the major issue with the developed indicator in this study is that it is only a rough estimate of the longitudinal functional connectivity at a large scale because it cannot reflect the differences in water level fluctuations between areas inside and outside of floodgates or in the different parts of a river channel, which means that this indicator cannot estimate longitudinal functional connectivity at the micro scale. Another limitation of the developed indicator is that it is a measurement of only the longitudinal functional connectivity of river systems, but functional connectivity is a four-dimensional concept including lateral, longitudinal, vertical, and temporal connectivity (Amoros and Bornette, 2010; Covino, 2017). Thus, the characteristic indicator of longitudinal functional connectivity should be further improved by combining more experimental observations at the micro scale. Furthermore, the measurement of functional connectivity should be synthetically investigated in the lateral, longitudinal, vertical, and temporal dimensions in the future.

4.2. Changes in longitudinal functional connectivity

In recent years, the river network connectivity of the Jiaxing Plain was also assessed using a comprehensive evaluation model based on hydraulic resistance and graph theory (Xu et al., 2012). Xu's result indicated that the river network connectivity was improved slightly after dredging; i.e., the river network connectivity increased from 0.0018 to 0.0028 between the 1960s and 2010s. The change trend of connectivity in his study was consistent with that in our study, but the change rate in his study was larger than that in ours. A primary reason for this difference is that the impacts of floodgates on river network connectivity were neglected in his study. However, the hydraulic connections between areas inside and outside of floodgates are limited extensively in delta plains. As a result, longitudinal functional connectivity depends largely on the control of floodgates in these regions. Therefore, the developed indicator in our study can more objectively reveal the actual condition of the longitudinal functional connectivity and thus can provide a reference for longitudinal functional connectivity assessment in other delta plains.

Our results also indicated that the longitudinal functional connectivity in YCDM was more positive than those in HJH and WCXY and that the value in the non-flood season was better than that in the flood season, but the abrupt changes in longitudinal functional connectivity presented larger difference in different subregions and stations, which was consistent with the observed facts. Longitudinal structural connectivity of river systems is the prerequisite for and foundation of longitudinal functional connectivity because hydrological processes depend on various rivers and lakes in delta plains. However, a study concerning river health assessments in these regions indicated that the longitudinal structural connectivity in YCDM was more positive than those in HJH and WCXY (Deng et al., 2015a). As an example, the γ index (i.e., network connectivity) of the arterial river systems was 0.54 in YCDM but was only 0.43 in HJH and WCXY. Therefore, compared with HJH and WCXY, better longitudinal structural connectivity led to preferable longitudinal functional connectivity in YCDM.

As mentioned, frequent flood disasters are a key environmental problem in the Taihu Plain (Wang et al., 2011). To mitigate flood disasters, thousands of floodgates were constructed across urban and rural areas. However, closed floodgates often generated independent rivers and lakes and cut off the original longitudinal functional connectivity of river systems. This conscious behavior by humans was extremely common during the flood season. Generally, these floodgates in urban areas and polders were closed to protect against the ingress of outer river floods during the flood season. In contrast, these floodgates were often opened to generate water exchanges between inner and outer river channels and lakes during the non-flood season. Consequently, the longitudinal functional connectivity during the non-flood season was always more positive than that during the flood season.

After the establishment of New China in 1949, most of the arterial river channels in the Taihu Plain were dredged, and numerous farmlands were also reverted to lakes. These human behaviours impacting increasing longitudinal functional connectivity became more common after the end of the 1970s. Therefore, the annual average value of longitudinal functional connectivity exhibited an abrupt increase in 1978. However, the sharp decrease in tributaries and the massive construction of floodgates also led to a decrease in longitudinal functional connectivity during the rapid urbanization. Thus, the changes in longitudinal functional connectivity during a certain period or in a certain region depended on these human behaviours. Specifically, longitudinal functional connectivity would be improved when protective behaviours were more vigorous than disruptive behaviours, whereas connectivity might decline otherwise. Moreover, the times and extents of these human behaviours were also characterized by significant differences in different subregions and at stations. Therefore, the times and trends of the abrupt changes in longitudinal functional connectivity were also entirely different in different subregions and stations.

Overall, a slight improvement in longitudinal functional connectivity in the Taihu Plain was observed in our results. In spite of this, the status of the longitudinal functional connectivity of this region was not ideal, especially at those stations near the borders of adjacent subregions. The results agreed with the actual situation in the Taihu Plain. To control floods, extensive water conservancy projects were constructed in each subregion in recent decades. Although these protective behaviours improved the longitudinal functional connectivity to some extent, they were effective in only some areas because of the lack of unified planning at the watershed scale. In recent years, the dramatic decrease in river systems under rapid urbanization (Deng et al., 2015b) led to the degeneration of longitudinal functional connectivity. Moreover, integrated watershed management in this region is not easy to implement due to the conflicting interests of flood disaster mitigation and water environmental protection of different subregions and cities.

Specifically, YCDM belongs to Suzhou City of Jiangsu Province, and WCXY belongs to Suzhou, Changzhou and Wuxi Cities of Jiangsu Province, but HJH belongs to Suzhou City of Jiangsu Province and Jiaxing, Huzhou and Hangzhou Cities of Zhejiang Province. Thus, the improvement of the longitudinal functional connectivity at those stations near the borders between adjacent subregions was often intentionally neglected by the local authorities on both sides. As a result, the longitudinal functional connectivity at these stations was less than those at the stations within each subregion.

5. Conclusions

In this study, according the differences between water level fluctuations at adjacent hydrological stations, we develop a new quantitative longitudinal functional connectivity index (LFCI) for delta plains. Focusing on the Taihu Plain, we then analyse the spatial-temporal changes in the LFCI during 1960–2012 and investigate the correlation between the LFCI and climate change and human activities. The analyses of these changes on LFCI lead to the following conclusions:

(1) The decadal, annual, and seasonal changes in the average LFCI all presented slightly increasing trends in the Taihu Plain. The average LFCI in the flood season was worse than that in the non-flood season, and those in June, July, and August were also worse than those in other months.
(2) The average LFCI was the least in WCXY, but those in YCDM during the flood season and in HJH during the non-flood season showed slightly decreasing trends. Decreasing trends were also present in June, July and August in YCDM and in the first three months and the last two months in HJH.
(3) The average LFCIs at those stations near the borders of adjacent subregions were less than those at other stations, and they all presented slightly decreasing trends. The average LFCI during the flood season was worse than that during the non-flood season at each station.
(4) Abrupt change analysis indicated that a significant increasing trend in the annual average LFCI in the Taihu Plain after 1978, but larger differences appeared between the times and trends of abrupt changes in the average LFCI at the subregional and station scales.
(5) Pearson correlation analysis showed that the average LFCI had a significant and negative correlation with the annual precipitation and significant and positive correlations with river density and water surface ratio but an insignificant and positive correlation with the number of floodgates.

According the above analysis, we believe the indicator developed in this study can be used as a practical tool to quantify the longitudinal functional connectivity of river systems in delta plains. Meanwhile, in order to improve the longitudinal functional connectivity of river systems, we also recommend that tributaries and lakes should be protected against reduction, that river channels should be dredged constantly, and that floodgates and other water conservancy projects should be controlled reasonably during rapid urbanization, especially in June, July and August in the flood season and at those stations near the borders of adjacent subregions.

Acknowledgements

This research work was financially supported by National Natural Science Foundation of China (Grant Nos. 41601039, 41771032, 41601018, 41807163, and 41301029), the National Key Research and Development Program of China (Grant No. 2016YFC0401502), and the Natural Science Foundation of Guangxi Province, China (Grant No. 2017GXNSFAA198012).

References

Ala-Aho, P., Soulsby, C., Pokrovsky, O.S., Kirpotin, S.N., Karlsson, J., Serikova, S., Vorobyev, S.N., Manasypov, R.M., Loiko, S., Tetzlaff, D., 2018. Using stable isotopes to assess surface water source dynamics and hydrological connectivity in a high-latitude wetland and permafrost influenced landscape. J. Hydrol. 556, 279–293.
Amoros, C., Bornette, G., 2010. Connectivity and biocomplexity in waterbodies of riverine floodplains. Freshw. Biol. 47 (4), 761–776.
Antoine, M., Javaux, M., Bielders, C., 2009. What indicators can capture runoff-relevant connectivity properties of the micro-topography at the plot scale? Adv. Water Resour. 32 (8), 1297–1310.
Bracken, L.J., Croke, J., 2007. The concept of hydrological connectivity and its contribution to understanding runoff-dominated geomorphic systems. Hydrol. Process. 21 (13), 1749–1763.
Bracken, L.J., Wainwright, J., Ali, G.A., Tetzlaff, D., Smith, M.W., Reaney, S.M., Roy, A.G., 2013. Concepts of hydrological connectivity: research approaches, pathways and future agendas. Earth Sci. Rev. 119, 17–34.
Cabezas, A., Gonzalez-Sanchís, M., Gallardo, B., Comín, F.A., 2011. Using continuous surface water level and temperature data to characterize hydrological connectivity in riparian wetlands. Environ. Monit. Assess. 183 (1–4), 485–500.
Caruso, B.S., 2015. A hydrologic connectivity index for jurisdictional analysis of headwater streams in a montane watershed. Environ. Monit. Assess. 187 (10), 1–23.
Chi, S., Wei, C., Zheng, J., Hu, J., Li, M., Hu, J., 2018. Distribution patterns of macroinvertebrate communities in a Chinese floodgate-regulated river and their relationships with river longitudinal connectivity. Sci. Total Environ. 631, 765–777.
Covino, T., 2017. Hydrologic connectivity as a framework for understanding biogeochemical flux through watersheds and along fluvial networks. Geomorphology 277, 133–144.
Deng, X., Xu, Y., Han, L., Yu, Z., Yang, M., Pan, G., 2015a. Assessment of river health based on an improved entropy-based fuzzy matter-element model in the taihu plain, china. Ecol. Ind. 57, 85–95.
Deng, X., Xu, Y., Han, L., Song, S., Yang, L., Li, G., Wang, Y., 2015b. Impacts of urbanization on river systems in the Taihu region, China. Water 7 (4), 1340–1358.
Deng, X., Xu, Y., Han, L., 2018. Impacts of human activities on the structural and functional connectivity of a river network in the Taihu Plain. Land Degrad. Dev. 29 (8), 2575–2588.
Duan, H., Ma, R., Xu, X., Kong, F., Zhang, S., Kong, W., Hao, J., Shang, L., 2009. Two-decade reconstruction of algal blooms in China's Lake Taihu. Environ. Sci. Technol. 43 (10), 3522–3528.
Good, S.P., Noone, D., Bowen, G., 2015. Hydrologic connectivity constrains partitioning of global terrestrial water fluxes. Science 349 (6244), 175–177.
Han, L., Xu, Y., Pan, G., Deng, X., Hu, C., Xu, H., Shi, H., 2015. Changing properties of precipitation extremes in the urban areas, Yangtze River Delta, China, during 1957–2013. Nat. Hazards 79 (1), 437–454.
Jaeger, K.L., Olden, J.D., Pelland, N.A., 2014. Climate change poised to threaten hydrologic connectivity and endemic fishes in dryland streams. Proc. Natl. Acad. Sci. 111 (38), 13894–13899.
Karim, F., Dutta, D., Marvanek, S., Petheram, C., Ticehurst, C., Lerat, J., Kim, S., Yang, A., 2015. Assessing the impacts of climate change and dams on floodplain inundation and wetland connectivity in the wet–dry tropics of northern Australia. J. Hydrol. 522, 80–94.
Liang, L., Li, L., Liu, Q., 2011. Precipitation variability in Northeast China from 1961 to 2008. J. Hydrol. 404 (1–2), 67–76.
Liu, L., Xu, Z.X., Reynard, N.S., Hu, C.W., Jones, R.G., 2013. Hydrological analysis for water level projections in Taihu Lake, China. J. Flood Risk Manage. 6 (1), 14–22.
Lu, C., Jia, Y., Jing, L., Zeng, Q., Lei, J., Zhang, S., Lei, G., Wen, L., 2018. Shifts in river-floodplain relationship reveal the impacts of river regulation: a case study of Dongting Lake in China. J. Hydrol. 559, 932–941.
Ma, Z., Kang, S., Zhang, L., Tong, L., Su, X., 2008. Analysis of impacts of climate variability and human activity on streamflow for a river basin in arid region of northwest China. J. Hydrol. 352 (3), 239–249.
Michaelides, K., Chappell, A., 2009. Connectivity as a concept for characterising hydrological behaviour. Hydrol. Process. 23 (3), 517–522.
Nilsson, C., Reidy, C.A., Dynesius, M., Revenga, C., 2005. Fragmentation and flow regulation of the world's large river systems. Science 308 (5720), 405–408.
Okin, G.S., Heras, M.M.D.L., Saco, P.M., Throop, H.L., Vivoni, E.R., Parsons, A.J., Wainwright, J., Peters, D.P., 2015. Connectivity in dryland landscapes: shifting concepts of spatial interactions. Front. Ecol. Environ. 13 (1), 20–27.
Pringle, C., 2003. What is hydrologic connectivity and why is it ecologically important? Hydrol. Process. 17 (13), 2685–2689.
Pumo, D., Arnone, E., Francipane, A., Caracciolo, D., Noto, L.V., 2017. Potential implications of climate change and urbanization on watershed hydrology. J. Hydrol. 554, 80–99.
Ramulifho, P.A., Rivers-Moore, N.A., Dallas, H.F., Foord, S.H., 2018. A conceptual framework towards more holistic freshwater conservation planning through incorporation of stream connectivity and thermal vulnerability. J. Hydrol. 556, 173–181.
Rinderer, M., Ali, G., Larsen, L., 2018. Assessing structural, functional and effective hydrologic connectivity with brain neuroscience methods: state-of-the-art and research directions. Earth Sci. Rev. 178, 29–47.
Smith, M.W., Bracken, L.J., Cox, N.J., 2010. Toward a dynamic representation of hydrological connectivity at the hillslope scale in semiarid areas. Water Resour. Res. 46 (12), 65–74.
Solà, C., Ordeix, M., Pou-Rovira, Q., Sellarès, N., Queralt, A., Bardina, M., Casamitjana, A., Munné, A., 2011. Longitudinal connectivity in hydromorphological quality

assessments of rivers. The ICF index: a river connectivity index and its application to Catalan rivers. Limnetica 30 (2), 273–292.
Stone, R., 2011. China aims to turn tide against toxic lake pollution. Science 333 (6047), 1210–1211.
Tang, B., Tong, L., Kang, S., Zhang, L., 2011. Impacts of climate variability on reference evapotranspiration over 58 years in the Haihe river basin of north China. Agric. Water Manage. 98 (10), 1660–1670.
Troch, P.A., Carrillo, G.A., Heidbüchel, I., Rajagopal, S., Switanek, M., Volkmann, T.H., Yaeger, M., 2009. Dealing with landscape heterogeneity in watershed hydrology: a review of recent progress toward new hydrological theory. Geography Compass 3 (1), 375–392.
Turnbull, L., Wainwright, J., Brazier, R.E., 2008. A conceptual framework for understanding semi-arid land degradation: ecohydrological interactions across multiple-space and time scales. Ecohydrology 1 (1), 23–34.
Wang, L., Cai, Y., Chen, H., Daler, D., Zhao, J., Yang, J., 2011. Flood disaster in Taihu Basin, China: causal chain and policy option analyses. Environ. Earth Sci. 63 (5), 1119–1124.
Wohl, E., Magilligan, F.J., Rathburn, S.L., 2017. Introduction to the special issue: Connectivity in Geomorphology. Geomorphology 277, 1–5.
Wu, C.L., Chau, K.W., Li, Y.S., 2009. Methods to improve neural network performance in daily flows prediction. J. Hydrol. 372 (1–4), 80–93.
Xie, P., Wu, Z., Sang, Y.F., Gu, H., Zhao, Y., Singh, V.P., 2018. Evaluation of the significance of abrupt changes in precipitation and runoff process in China. J. Hydrol. 560, 451–460.
Xu, G., Xu, Y., Wang, L., 2012. Evaluation of river network connectivity based on hydraulic resistance and graph theory. Adv. Water Sci. 23 (6), 776–781.
Yaghmaei, H., Sadeghi, S.H., Moradi, H., Gholamalifard, M., 2018. Effect of Dam operation on monthly and annual trends of flow discharge in the Qom Rood Watershed, Iran. J. Hydrol. 557, 254–264.
Zhao, F.F., Xu, Z.X., Huang, J.X., Li, J.Y., 2008. Monotonic trend and abrupt changes for major climate variables in the headwater catchment of the Yellow River basin. Hydrol. Process. 22 (23), 4587–4599.